Performance Evaluation of an Entry Research Vehicle

Richard W. Powell,* J. Chris Naftel,* and Mark J. Cunningham*
NASA Langley Research Center, Hampton, Virginia

An entry research vehicle is being proposed as a candidate Shuttle-launched flight experiment. This vehicle would be used to demonstrate maneuverability in the atmosphere, test advanced thermostructure concepts, and measure the atmospheric flight conditions encountered by the vehicle. Two types of missions would be performed by this vehicle. The first are those maneuvers required to generate the downrange and crossrange required for entry. The second is a synergetic plane change. These missions will provide a data base to validate analytical prediction techniques. This paper will discuss these two maneuvers.

Nomenclature

ADDB = Aerodynamic Design Data Book
APAS = Aerodynamic Preliminary Analysis System
b = reference span, ft
C = Chapman-Rubesin viscosity coefficient
C_D = drag coefficient = drag/qS
C_L = lift coefficient = lift/qS
C_l = rolling-moment coefficient = rolling moment/qSb
C_{l_β} = $\delta C_l/\delta_\beta$, deg^{-1}
C_m = pitching-moment coefficient = pitching moment/qSl
C_n = yawing-moment coefficient = yawing moment/qSb
C_{n_β} = $\delta C_n/\delta\beta$, deg^{-1}
ERV = Entry Research Vehicle
HABP = Hypersonic Arbitrary Body Program
h = altitude, ft
ISP = specific impulse, s
l = reference length, ft
L/D = C_L/C_D
LHHT = Langley Hypersonic Helium Tunnel
M = Mach number
q = dynamic pressure, psf
q = convective heat rate, BTU/ft^2-s
Re = Reynolds number
S = reference area, ft^2
UDP = Unified Distributed Pressure
$\bar{V}'_\infty$ = viscous correlation parameter = $M\sqrt{C}/\sqrt{Re}$
α = angle of attack, deg
β = sideslip angle, deg
δ_{BF} = body-flap deflection, deg
δe = elevator deflection, deg
ΔC_L = C_L increment
ΔV = ideal velocity increment, ft/s

Introduction

NOW that the Space Shuttle is operational, interest is turning to the development of other reusable space transportation system elements to provide additional operational flexibility. One area is to develop the capability for increased maneuvering within the atmosphere. Some uses for this capability are to provide an overflight of an intermediate point during entry, increase the landing footprint, or perform a synergetic plane change. The Shuttle flights have made entry from low-Earth orbit routine, but data obtained from the Shuttle flights have established a somewhat restricted data base. Operational and safety requirements have significantly constrained the orbiter entry profile available for flight data measurement. The development of entry vehicles that effectively use aerodynamic forces and moments to maneuver will dictate a need for a major advancement in technology over the current Shuttle orbiter. Because of this requirement for significant advancements over existing technology, an entry flight experiment is being proposed. This experiment would provide a data base to assess the new technology required to support the development of a maneuvering entry vehicle. These technologies would include thermal protection system materials, lightweight structural concepts, and advanced avionics.

A high-performance vehicle is required for maneuvering entry. Significant technology improvements must be made before such a vehicle is feasible. Aerodynamic and aeroheating flight data will provide the technology base required to reduce the aerodynamic uncertainty level and provide accurate design data. Providing the technology base to reduce conventional TPS and material design margins would allow the necessary weight reductions to enable the serious consideration of an operational vehicle with large atmospheric maneuvering capability.

One configuration that is proposed for the entry flight experiments is known as the Entry Research Vehicle (ERV). This concept is designed to be deployed by the Space Shuttle Orbiter while in orbit. Once the orbiter has reached a safe separation distance, the ERV will deorbit and perform its mission. Two types of missions have been proposed for the ERV. These are an entry involving both angle-of-attack and bank-angle modulation, and a synergetic plane change. A synergetic plane change is a maneuver that combines aerodynamic and propulsive forces to change the inclination and nodes of the orbit. This method can produce these orbital changes for less fuel than would be required for an all-propulsive maneuver.

Configuration

The Entry Research Vehicle is 25 ft long and has a wing span of 13 ft. It is designed to occupy half of the Shuttle cargo bay, which is 60 ft long and 15 ft in diameter. The configuration has a distinct wing-body design with a blended wing-body interface to increase the overall hypersonic performance of the vehicle. The wing has a reference area of 177.4 ft^2. The reference length used to determine C_m was the vehicle length, 25 ft. Elevons are used for pitch control, ailerons are used for roll control, and tip-fin controllers will provide yaw control. A body flap assists in trimming the vehicle in pitch. Reaction control system thrusters will be needed to control the vehicle on orbit and in the upper atmosphere. The thrusters will be placed in the nose of the vehicle and in the tip fins.

Presented as Paper 86-0270 at the AIAA 24th Aerospace Science Meeting, Reno, NV, Jan. 6-9, 1986; received June 12, 1986; revision received Feb. 19, 1987.

*Aerospace Engineer, Space Systems Division. Member AIAA.

Figure 1 is a three-view drawing of the ERV showing the basic vehicle dimensions and the control surfaces. The fineness ratio of the fuselage is approximately 6, and its volume is 300 ft.[3] Figure 2 shows an inboard profile of the ERV. The payload bay that will house many of the experiments will be placed in the nose of the vehicle, where atmospheric sensing can be performed with minimal engine combustion by-product contamination. The avionics will be located behind the payload compartment. To minimize the center-of-gravity shift with propellant depletion, the fuel and oxidizer tanks are positioned around the c.g., which is located at 67% of the body length. The electrical system and batteries are positioned between the fuel tanks, approximately at the c.g. Propulsion is provided by three Marquardt R-40-B rocket motors, each providing 1100 lb of thrust with an ISP of 295 s.

The launch weight of the ERV from the Space Shuttle is 12,000 lb of which 6,000 lb is propellant. A weight summary is shown in Table 1.

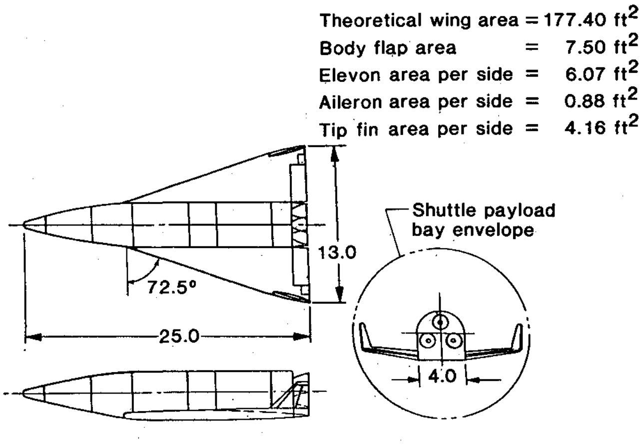

Fig. 1 Three-view drawing of the ERV.

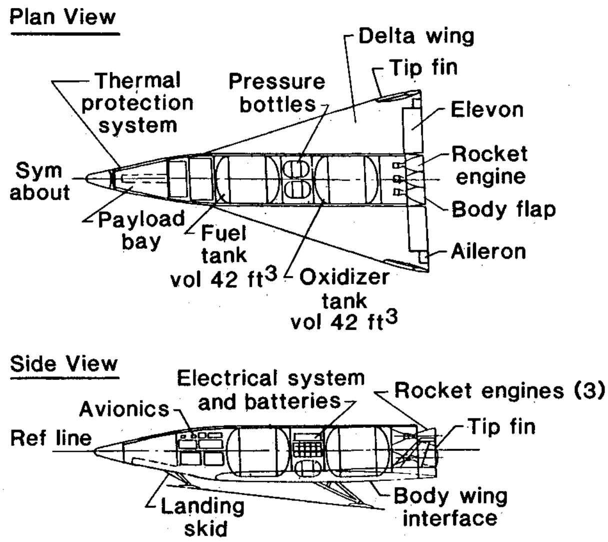

Fig. 2 Inboard profile of the ERV.

Aerodynamic Overview

An aerodynamic data base was compiled for the ERV through a combination of theoretical predictions, wind-tunnel data, and experience from the Shuttle program. Aerodynamic data from the Space Shuttle Aerodynamic Design Data Book (ADDB)[2] were used to complete the ERV aerodynamic data base where wind-tunnel data were not available and reliable analytical predictions could not be obtained. Figure 3 outlines this process. As shown in this figure, the role of the aerodynamic data base during the design process is to provide the aerodynamic characteristics for trajectory and performance analyses and, in particular, to study the missions presented herein.

Wind-tunnel data for this configuration are limited to a force-and-moment test in the Langley Hypersonic Helium Tunnel (LHHT). The model was tested with an adjustable body flap at a Mach number of 20.35 and a Reynolds number per foot of 6.8×10^6 in helium. These conditions simulate Mach-10 flight in air for a 25-ft vehicle at an altitude of 145,000 ft. The longitudinal test data are presented in Ref. 3, and the lateral-directional and the body flap control effectiveness test data will be presented in this report.

An entry vehicle such as the ERV is required to fly in various flight regimes. Three distinct flight regimes can be identified as the continuum, the transition, and the free-molecule regimes. Therefore, various techniques are used to assess the aerodynamics within the different flight regimes. The continuum regime includes the subsonic, supersonic, and hypersonic speed ranges. The viscous interaction regime is characterized as that part of the continuum where viscous effects have a dominant effect on the vehicle aerodynamics. The transition regime is characterized by a large change in the Knudsen number, which is defined as the ratio of the mean free path of the molecules to a characteristic length of the vehicle. Using the fuselage length of the ERV, the transition regime starts at a Knudsen number of 0.001 and ends at a Knudsen number of 10. The free-molecule regime is characterized by Knudsen numbers greater than 10. In each flight regime, a unique parameter was chosen to correlate the aerodynamics. In the continuum, the Mach number was chosen. In the viscous interaction regime, the viscous correlation parameter $\bar{V}_\infty'$ was chosen. This parameter is defined and the criteria for its choice is discussed in Ref. 3. This parameter was used in the Space Shuttle ADDB. In the transition and free-molecule regime, altitude was chosen because it is a calculated parameter in the performance programs and it can be related to the Knudsen number.

The aerodynamics in the subsonic and supersonic continuum were analytically predicted with the Aerodynamic Preliminary Analysis System (APAS).[4] In the subsonic and supersonic regimes, the configuration was analyzed using the Unified Distributed Pressure (UDP) theory. This theory simulates the configuration by a distribution of source and vortex singularities, each of which satisfy the linearized small-perturbation potential equation of motion. The singularity strengths are obtained by satisfying the condition that the flow is tangent to the local surface. The velocities and pressures throughout the flow may be obtained from the singularity strengths. A thorough description of the program is presented in Ref. 4. The aerodynamic predictions in the

Table 1 Entry research vehicle weight summary

(all weights in pounds)	
Structure	2,930
Propulsion	420
Subsystems	1,740
Dry weight	5,090
Payload	500
Fuel	6,410
Launch weight	12,000

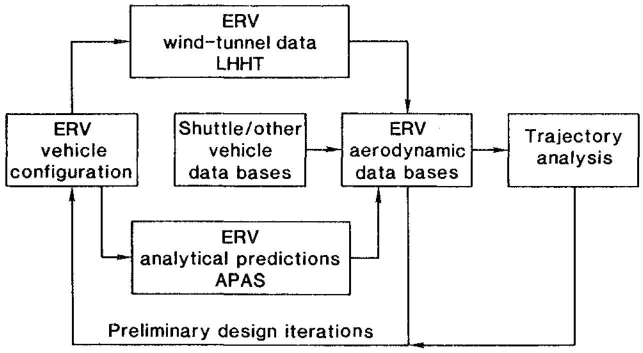

Fig. 3 Outline of procedure to obtain the aerodynamic data base for the ERV.

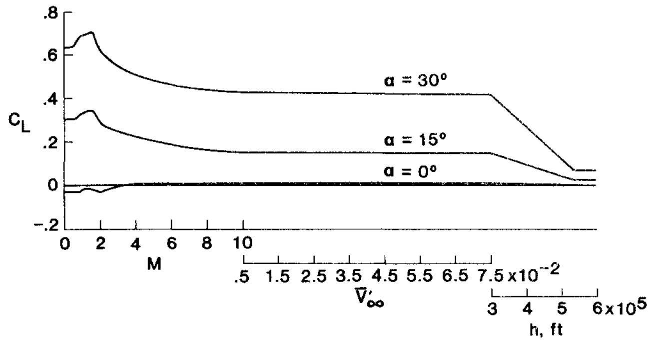

Fig. 4 Predicted C_L profile for the ERV.

hypersonic continuum, the viscous interaction regime, and the free-molecule regime were performed with the Hypersonic Arbitrary Body Program (HABP), which has been integrated into APAS. The HABP performs a noninterfering, constant-pressure, finite-element analysis. The configuration is approximated by a system of plane quadrilateral panels. The pressure acting on each panel is evaluated by a specified compression-expansion method. In the hypersonic continuum and the viscous interaction regimes, the Modified Newtonian Theory was used to analyze the panels. In the free-molecule regime, Newtonian Theory was used with normal and tangential accommodation coefficients. The technique to estimate the aerodynamics in the transition regime will be discussed in the next section. Reference 2 can provide additional details on the techniques and methods employed to predict the aerodynamics in the hypersonic continuum, the viscous interaction regime, the transition regime, and the free-molecule regime.

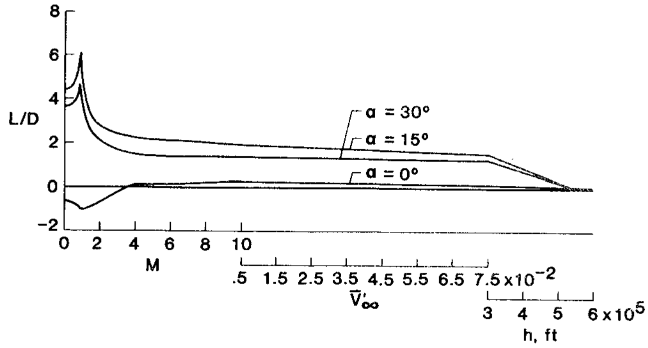

Fig. 5 Predicted L/D profile for the ERV.

Longitudinal Aerodynamics

The basic longitudinal characteristics such as the lift, drag, and pitching-moment coefficients were all predicted with APAS. The results were compared with the wind-tunnel data obtained in the LHHT, and the comparisons indicated that the APAS predictions were sufficiently accurate for developing the data base. The comparisons are illustrated in Ref. 3. The basic lift coefficient for the ERV configuration is presented in Fig. 4. This type of plot will be used to display many of the results, since it spans the various flight regimes and uses the appropriate correlation parameters as summarized earlier. The subsonic, supersonic, and hypersonic speed ranges in the continuum regime are distinguished on the plot by the use of the Mach number as the independent parameter. The viscous-interaction regime is denoted by the correlation parameter $\bar{V}'_\infty$. The transition regime starts at an altitude of ≈ 300,000 ft and ends at ≈ 537,000 ft. A linear bridging function between the viscous-interaction and free-molecule regimes was used to estimate the aerodynamics in the transition regime. However, for a more accurate estimation of the aerodynamics in this regime, a bridging formula such as the one presented in Ref. 3 should be used. The free-molecule regime commences at ≈ 537,000 ft and continues to higher altitudes. A common trend in this figure and later ones is that the particular coefficient will vary only slightly in the subsonic speed range, the hypersonic continuum, and the viscous-interaction regimes. However, at transonic speeds and in the transition regime, the coefficients vary significantly. The lift-to-drag ratio (Fig. 5) further exemplifies this point. Here, at 15 deg angle of attack, the maximum lift-to-drag ratio is slightly above 6.0 just below Mach 1.0 and drops to approximately 2.3 at Mach 1.05. There is a gradual decay of L/D in the hypersonic continuum and the viscous-interaction regimes where both the Mach number and $\bar{V}'_\infty$ are increasing, but a more rapid decay is seen in the transition regime.

A particular point of interest for performance studies is the maximum hypersonic lift-to-drag ratio. Based on the wind-tunnel results at a $\bar{V}'_\infty$ of 0.005, a maximum lift-to-drag of 1.9 was achieved at 16 deg angle of attack. This is also shown in Ref. 3.

Lateral-Directional Aerodynamics

Experimental data obtained in the LHHT for the ERV and Shuttle ADDB were used to estimate the lateral-directional aerodynamics for the ERV. The UDP theory calculates these aerodynamic characteristics in the subsonic to supersonic speed ranges. However, because of the absence of wind-tunnel data to support the predictions, these analytical predictions were not incorporated into the data base. At hypersonic speeds, the HABP also calculates the lateral-directional coefficients, but since the program currently does not account for shielding, the lateral-directional predictions are poor. Shielding refers to the phenomenon that if a hypersonic streamline encounters a panel upstream of another panel, then the pressure on the downstream panel should not contribute to the overall pressure on the body. Currently, the program incorporates the pressures on both the upstream and downstream panels. Therefore, the lateral-directional aerodynamics that were obtained in the LHHT (Fig. 6) were maintained as the characteristics in the viscous interaction regime, the transition regime, and the free-molecule regime. Below Mach 10, the Shuttle's lateral-directional characteristics were modified to estimate the aerodynamics for the ERV using the test data from the LHHT as a guide. Figures 7 and 8 illustrate the lateral stability (C_{l_β}) and the directional stability (C_{n_β}) coefficients in the continuum regime.

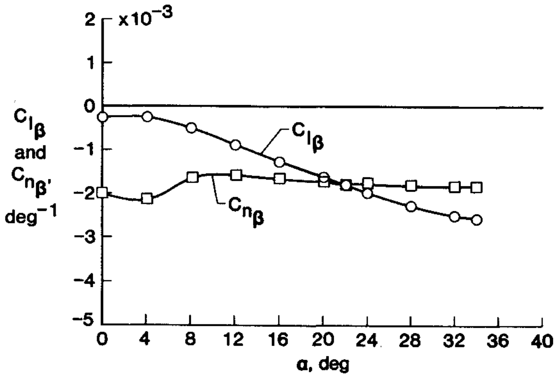

Fig. 6 Lateral-directional data obtained from NASA Langley Hypersonic Helium Tunnel tests of the ERV.

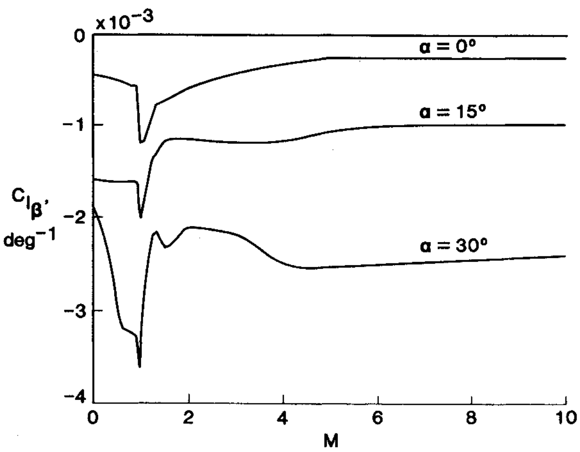

Fig. 7 C_{l_β} profile in the subsonic, supersonic, and hypersonic continuum.

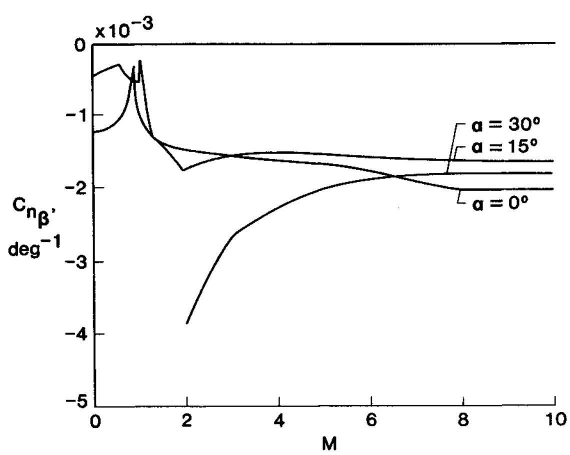

Fig. 8 C_{n_β} profile in the subsonic, supersonic, and hypersonic continuum.

Mission Analysis Technique

All the results that will be presented in the following section were generated by using the three-degree-of-freedom version of the Program to Optimize Simulated Trajectories (POST).[5] The POST program is a generalized event-oriented trajectory program and can be used to analyze ascent, on-orbit, and entry problems. The program can use any calculated variables as optimization and constraint parameters. The program optimizes one variable subjected to constraints. The maximum number of constraints is 25, and these can be either equality or inequality.

Missions

Studies of future space transportation needs have shown the desirability, from an improved operational flexibility standpoint, of a larger landing footprint than that of the Space Shuttle. In addition, the desirability for large orbital inclination changes has been shown. Many studies have shown that for large plane changes in low-Earth orbit, a synergetic plane change will use less fuel than an all-propulsive maneuver. The ERV is designed to demonstrate the technologies required to perform both the entry missions and the synergetic plane change mission. These missions are depicted in Fig. 9. Figure 10 shows the landing footprint of the ERV as compared with the Space Shuttle. To achieve this footprint requires that the ERV be able to fly a range of hypersonic angles of attack between 10 and 40 deg. In contrast, the Space Shuttle flies a single angle-of-attack profile for all missions. Figure 11 shows the altitude profiles for three ERV entry missions: maximum downrange, maximum crossrange, and minimum downrange. All ranges are calculated from the time the ERV reaches 400,000 ft. The trajectories are tailored so that the maximum convective heat rate referenced to a 1-ft radius sphere will not exceed 125 Btu/ft^2-s. The maximum downrange mission is performed by flying a constant angle of attack at a 0-deg bank angle. Because it is initially above the equilibrium glide slope, the ERV performs a skipping entry. Figure 12 shows the angle-of-attack profiles for the entry missions, and Fig. 13 shows the bank-angle profiles for the minimum downrange and maximum crossrange missions. Figure 14 shows the convective heat-rate profiles, and Fig. 15 shows the total heat load for the entry missions. The maximum downrange entry was tailored so that the total heat load would not exceed that of the maximum crossrange entry. This limits the maximum downrange; however, this is not a significant constraint, since the downrange can be augmented by delaying the deorbit burn.

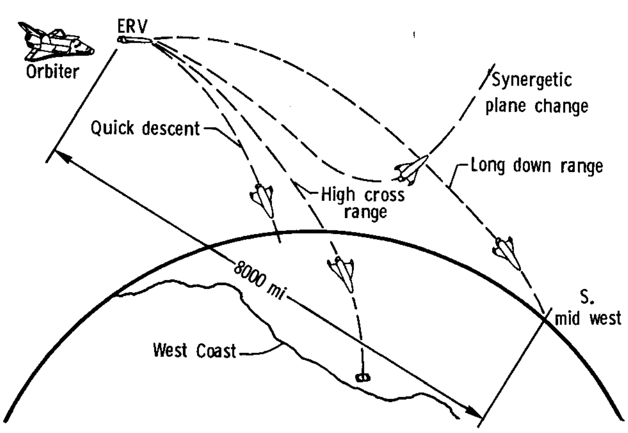

Fig. 9 Candidate missions for the ERV.

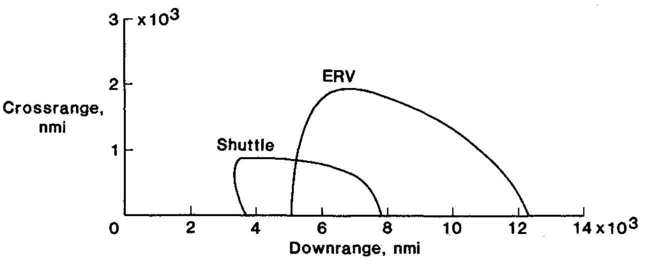

Fig. 10 Landing footprint comparison of the ERV and the Space Shuttle.

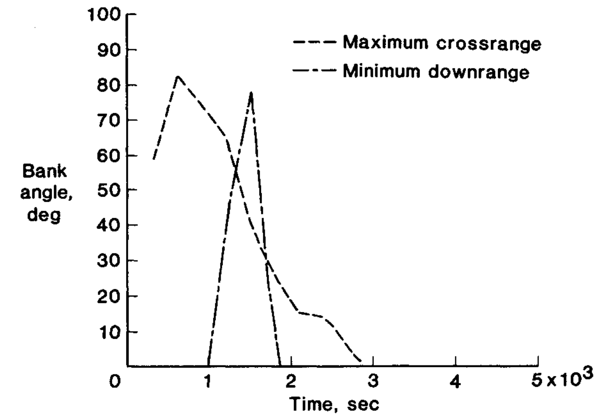

Fig. 13 Bank-angle profiles for the entry missions of the ERV.

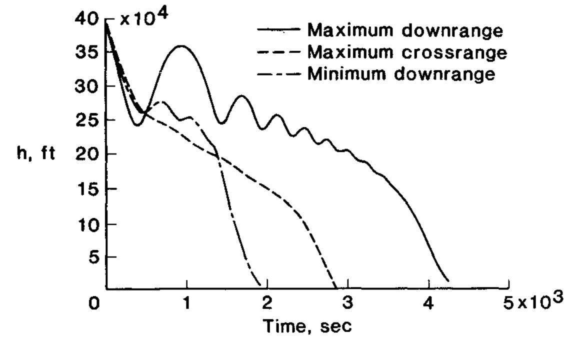

Fig. 11 Altitude profiles for the entry missions of the ERV.

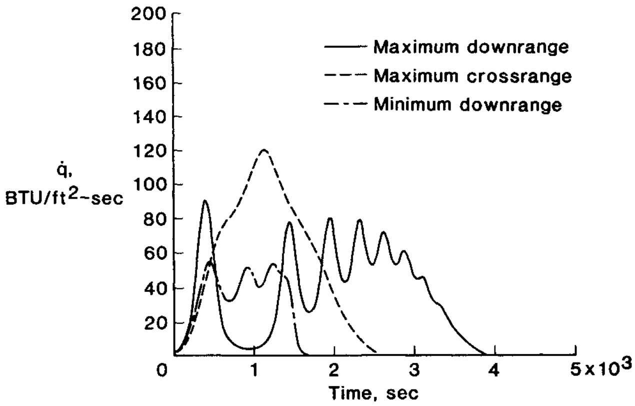

Fig. 14 Heating-rate profiles for the entry missions for the ERV.

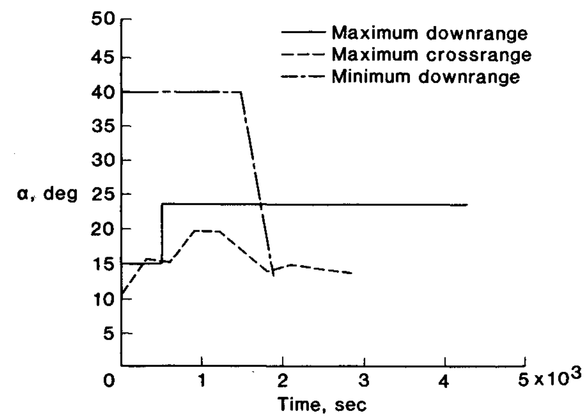

Fig. 12 Angle-of-attack profiles for the entry missions of the ERV.

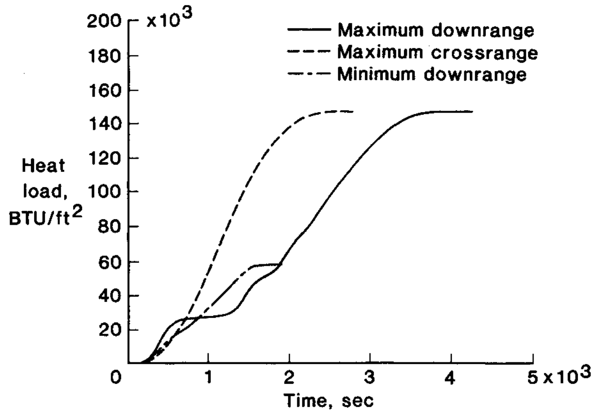

Fig. 15 Total heat-load profiles for the entry missions of the ERV.

The ΔV required to perform an orbital inclination change is shown in Fig. 16. Results are shown for an in-orbit, all-propulsive maneuver and for two synergetic plane change maneuvers, one constrained to a maximum convective heat rate referenced to a 1-ft radius sphere of 80 Btu/ft^2-s and one constrained to a maximum heat rate of 125 Btu/ft^2-s. The guidance strategy for both synergetic plane change maneuvers is similar. After the deorbit burn, the engines are shut down. Once the vehicle enters the atmosphere and the heating rate reaches the limit, the engines are restarted and throttled to maintain a constant velocity. At the end of this cruising phase the engines return to maximum thrust and the vehicle exits the atmosphere. Bank-angle control is used during the entire atmospheric pass so that part of the required inclination change occurs on the inbound and exit legs. The altitude, angle-of-attack, bank-angle engine throttling, heat rate, and heat-load histories are shown in Figs. 17–22 respectively. For the synergetic plane change with a design maximum convective heat rate of 80 Btu/ft^2-s, the ERV pulls out (altitude rate = 0 ft/s) at the design heating rate and the

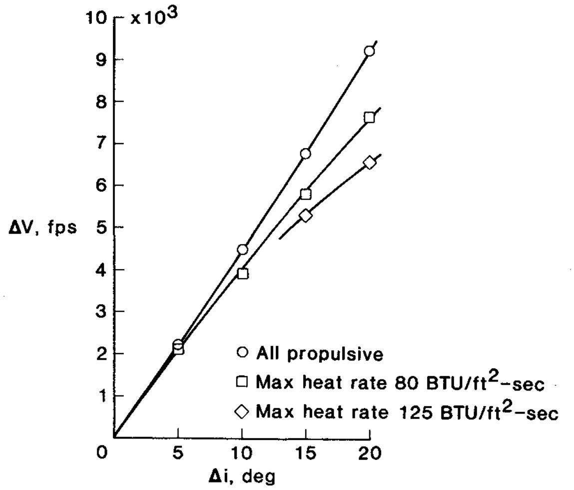

Fig. 16 Comparison of ΔV requirements for all-propulsive maneuvers and synergetic maneuvers to produce an orbital inclination change for the ERV.

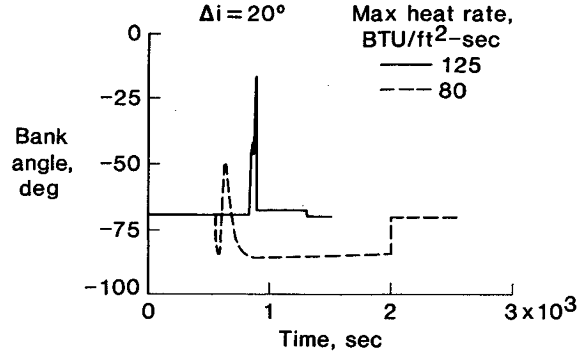

Fig. 19 Bank-angle profiles for synergetic plane changes for the ERV.

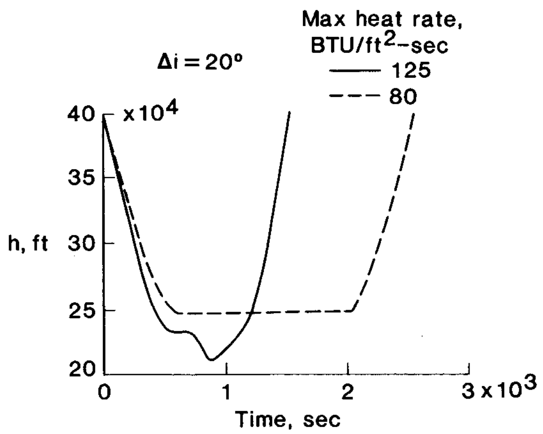

Fig. 17 Altitude profiles for synergetic plane changes for the ERV.

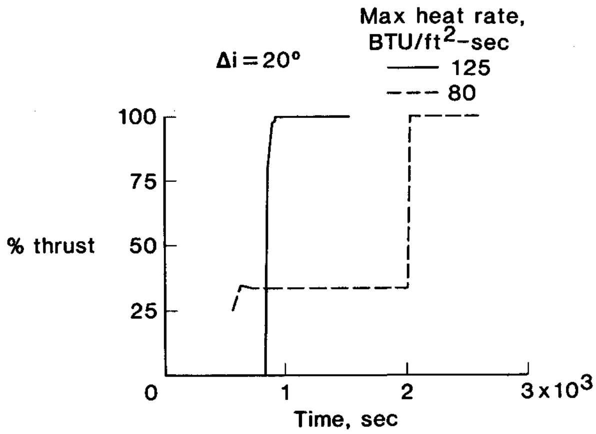

Fig. 20 Engine throttling profiles for synergetic plane changes for the ERV.

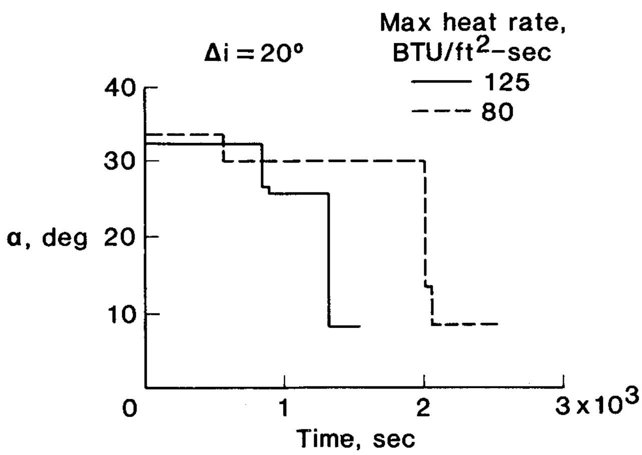

Fig. 18 Angle-of-attack profiles for synergetic plane changes for the ERV.

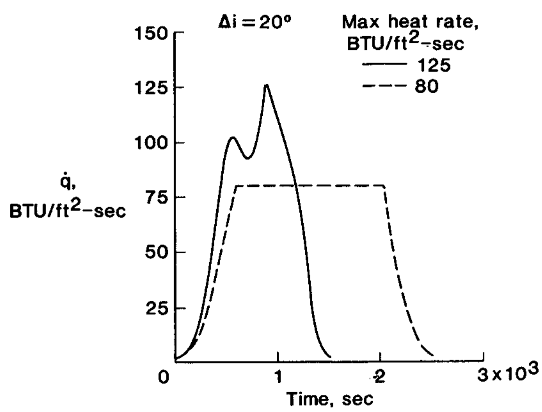

Fig. 21 Heating-rate profiles for synergetic plane changes for the ERV.

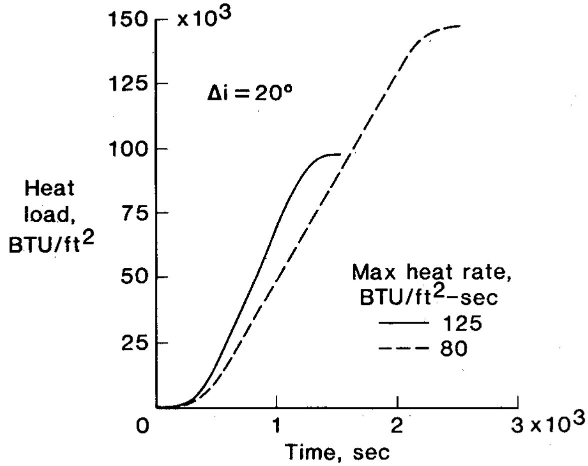

Fig. 22 Total heat-load profiles for synergetic plane changes for the ERV.

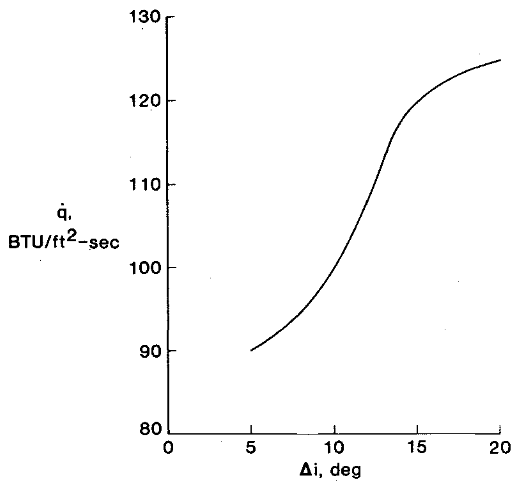

Fig. 23 Optimum convective heating rate for synergetic orbital inclination changes for the ERV.

engines are ignited. However, for the case with the design maximum heating rate of 125 Btu/ft^2-s, the ERV pulls out at a heating rate of $\approx$ 100 Btu/ft^2-s and continues to glide (engine off) until the design maximum heating rate is reached. Once the design maximum heating rate is reached, the engines are ignited. For this case, once the limit is reached, the exit maneuver begins almost immediately. By pulling out at 100 Btu/ft^2-s, the ERV uses the propulsion system only for a short cruise and the exit maneuver. If the vehicle pulls out at the 125 Btu/ft^2 limit, more fuel is expended because of the expanded cruise phase. Because almost all the plane change occurs on the inbound and exit legs, there is no advantage to raising the heating-rate limit above the 125 Btu/ft^2-s for a 20-deg inclination change. Thus, the heat-rate limit of 125 Btu/ft^2-s produces the most fuel-efficient 20-deg orbital inclination change for the ERV. This analysis was extended to find the optimum heating-rate limit for each desired plane change increment. The optimum is shown in Fig. 23.

Summary

A preliminary performance analysis has been completed for a proposed entry research vehicle concept that would be launched from the Space Shuttle. One objective of the flight experiment would be to provide the technology data base for future vehicles that have the requirement for atmospheric maneuvers more demanding than those of the Space Shuttle. An aerodynamic data base was compiled to perform the performance analysis. The results of the analysis showed that the landing footprint of the entry research vehicle is much larger than the Space Shuttle's and that the vehicle is capable of performing a synergetic maneuver producing a 20-deg orbital inclination change.

References

[1]Freeman, D.C., et al, "Definition of an Entry Research Vehicle," AIAA Paper 85-0969, June 1985.

[2]"Aerodynamic Design Data Book, Vol. 1—Orbiter Vehicle, STS-1," Rockwell International, SD72-SH-0060, Vol. 1M, 1980.

[3]Cunningham, M.J., "Aerodynamics for an Entry Research Vehicle," AIAA Paper 85-1793-CP, Aug. 1984.

[4]Bonner, E., Clever, W., and Dunn, K., "Aerodynamic Preliminary Analysis System II, Part I—Theory," NASA CR-165627, April 1981.

[5]Braver, G.L., Cornick, D.E., and Stevenson, R., "Capabilities and Applications of the Program to Optimize Simulated Trajectories (POST)," NASA CR-2770, Feb. 1977.